*Supporting Information*

# A Universal Synthesis Strategy for Stable $CsPbX_3$@Oxide Core-Shell Nanoparticles through Bridging Ligands

*Bing Tang,[a, b] Xuan Zhao,[a] Lin Ji Ruan,[a, b] Changyun Qin,[a] Ang Shu[a] and Ying Ma*[*a, b]*

[a] State Key Laboratory of Materials Processing and Die & Mould Technology, School of Materials Science and Engineering, Huazhong University of Science and Technology, Wuhan 430074, P. R. China

[b] Shenzhen Huazhong University of Science and Technology Research Institute, Shenzhen

**Corresponding Author**

**E-mail: yingma@hust.edu.cn*

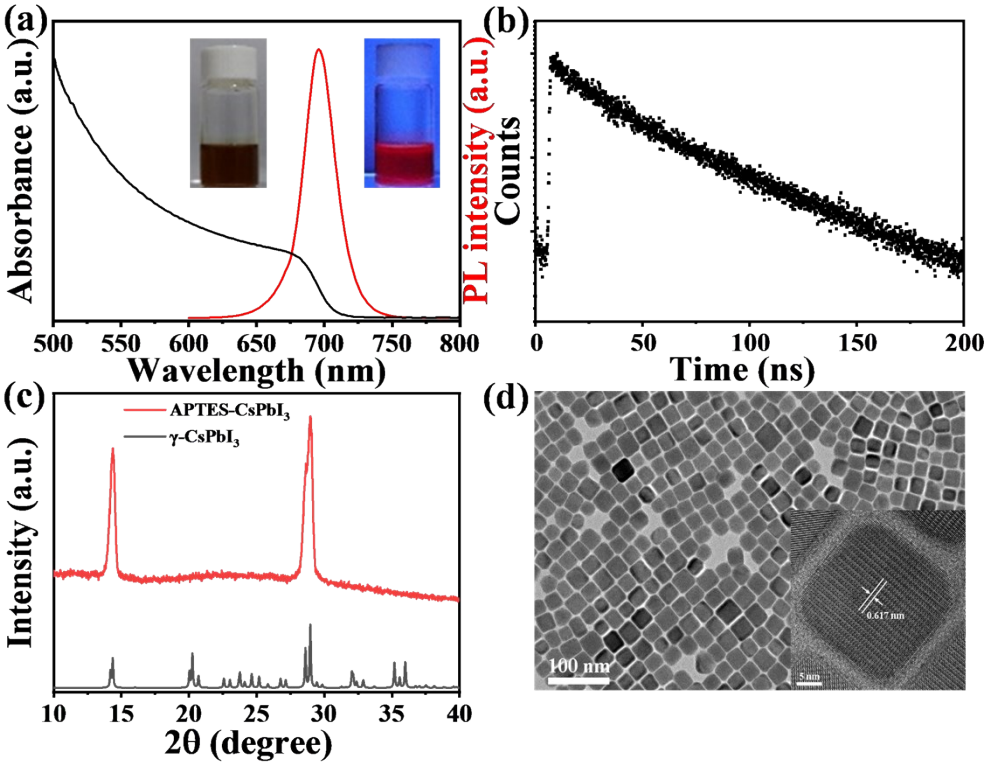


**Fig. S1** (a) PL spectrum and UV-Vis absorption spectrum of APTES-$CsPbI_3$ solution. The inset shows the APTES-$CsPbI_3$ solution under daylight and UV light irradiation ($\lambda$ = 365 nm). (b) Time-resolved PL decay, (c) XRD pattern and (d) TEM images of APTES-$CsPbI_3$ NCs.

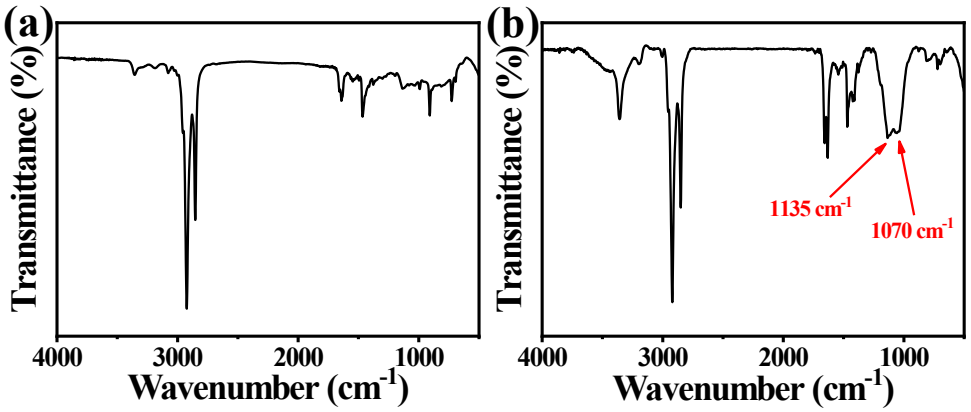


**Fig. S2** FT-IR spectra of (a) APTES-$CsPbI_3$ NCs and (b) $CsPbI_3$@$SiO_2$ NCs.

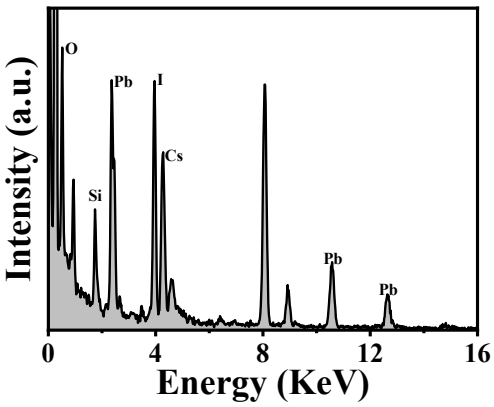


**Fig. S3** The energy-dispersive X-ray spectrum of the $CsPbI_3@SiO_2$ NCs.

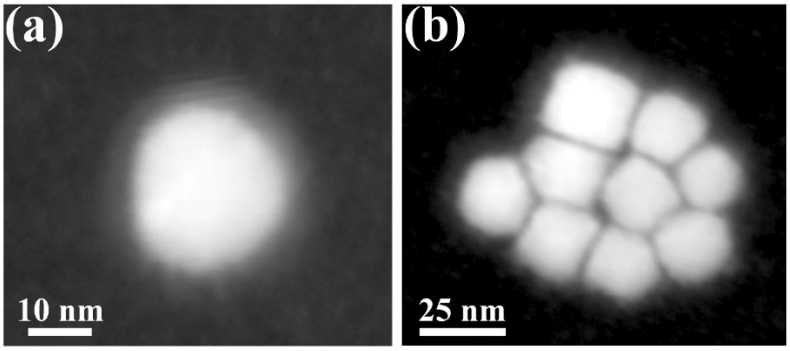


**Fig. S4** The HADDF-STEM images of the $CsPbI_3@SiO_2$ NCs.

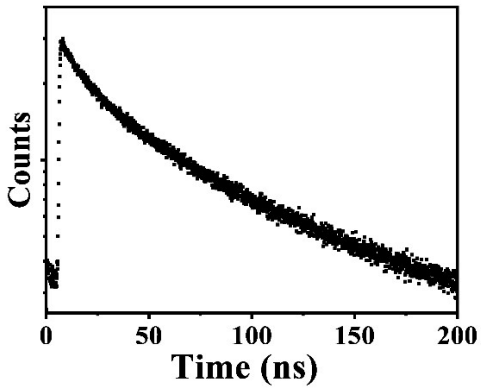


**Fig. S5** The time-resolved PL decay of the $CsPbI_3@SiO_2$ NCs.

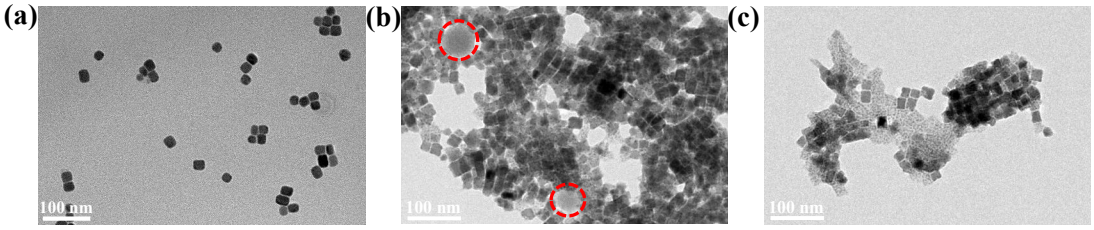


**Fig. S6** TEM images of the products prepared at different ammonia concentrations: (a) 3.4, (b) 6.7, and (c) 10 mmol $L^{-1}$.

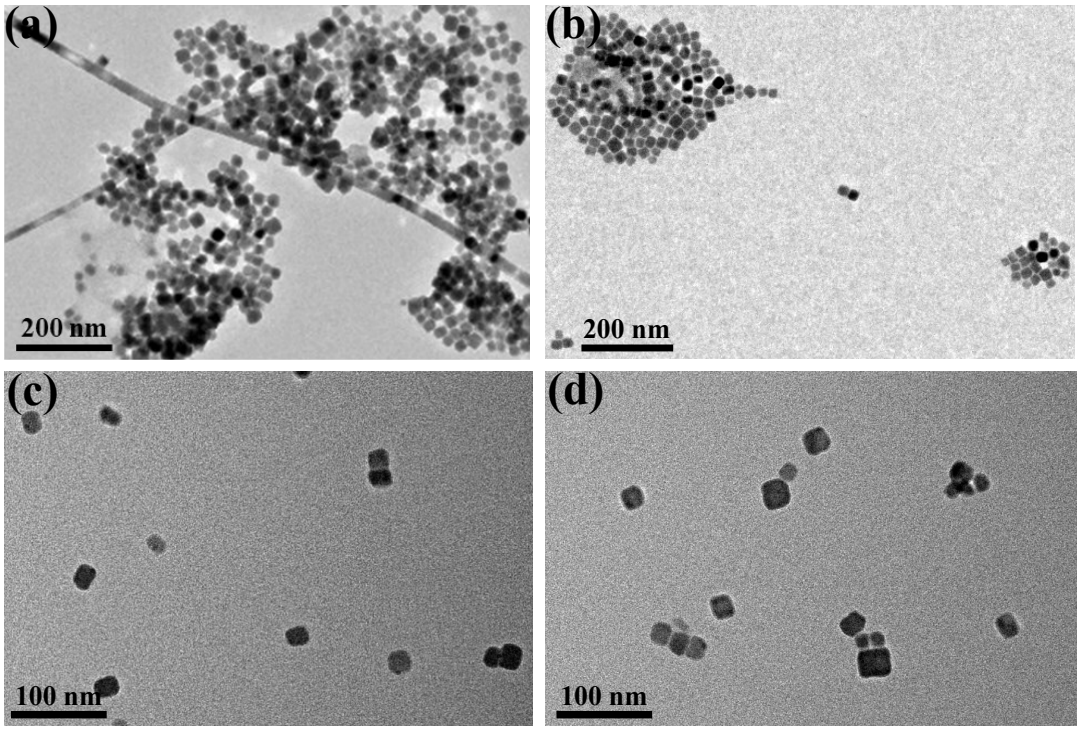


**Fig. S7** TEM images of the products prepared by varying ethanol quantities: (a) 0.5 mL, (b) 1 mL, (c) 2 mL, and (d) 3 mL.

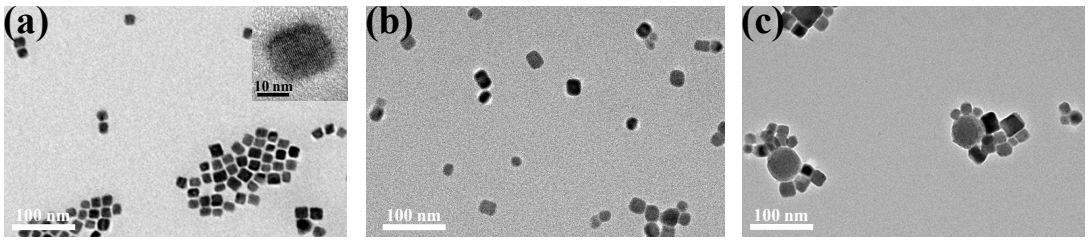


**Fig. S8** TEM images of the products prepared at different hydrolysis temperatures: (a) 20 °C, (b) 25 °C and (c) 30 °C.

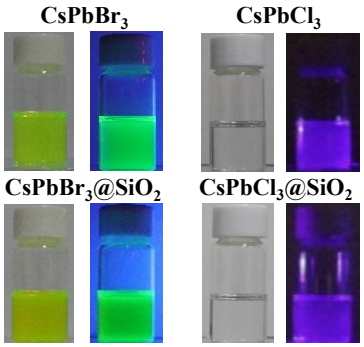


**Fig. S9** Photographs of the $CsPbBr_3$ and $CsPbCl_3$ NCs before and after $SiO_2$ shell growth under daylight and UV light irradiation ($\lambda$ = 365 nm).

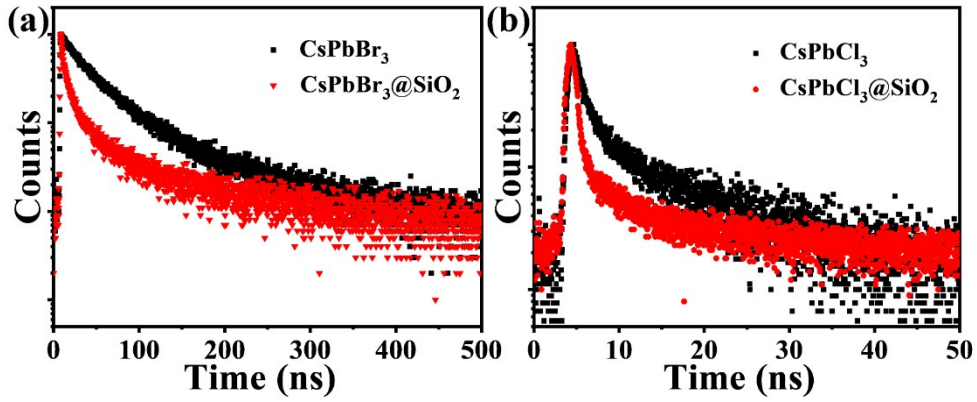


**Fig. S10** Time-resolved PL decay curves of (a) $CsPbBr_3$ and (b) $CsPbCl_3$ NCs before and after $SiO_2$ shell growth.

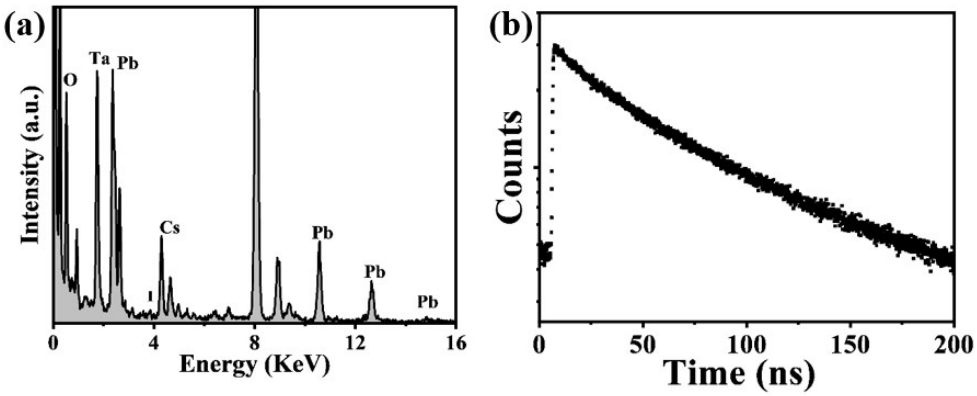


**Fig. S11** The energy-dispersive X-ray spectrum (a) and the time-resolved PL decay (b) of the $CsPbI_3@Ta_2O_5$ NCs.

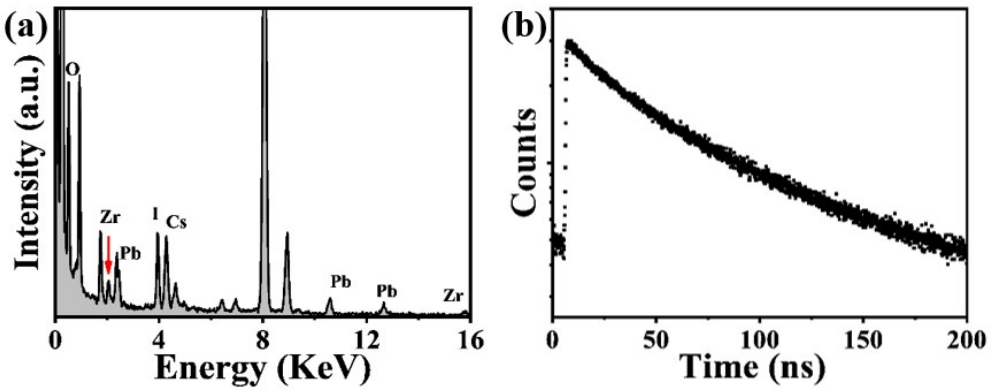


**Fig. S12** The energy-dispersive X-ray spectrum (a) and the time-resolved PL decay (b) of the $CsPbI_3$@$ZrO_2$ NCs.

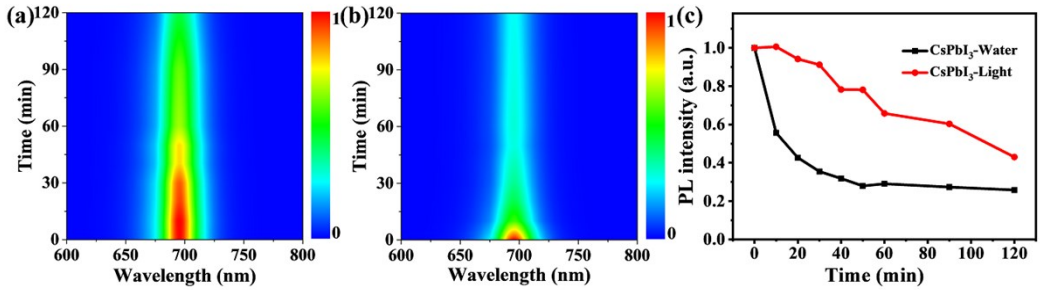


**Fig. S13** Pseudocolor map of PL spectra for APTES-$CsPbI_3$ NCs recorded at different time intervals after toluene dispersion is floated onto water forming a toluene/water interface. Pseudocolor map of PL spectra for APTES-$CsPbI_3$ NCs recorded at different time intervals after UV-light irradiation. (c) The corresponding integrated PL intensity as a function of time. The integrated PL intensity is normalized to the initial value.

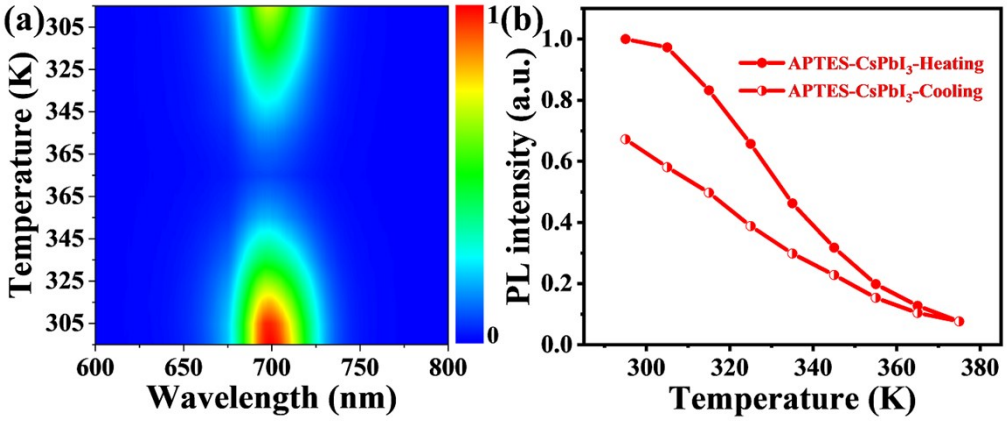


**Fig. S14** Pseudocolor map of temperature-dependent PL spectra for APTES-$CsPbI_3$ NCs via heating/cooling cycles from room temperature to 375 K. (b) The corresponding integrated PL intensity as a function of temperature. The integrated PL intensity is normalized to the initial value.

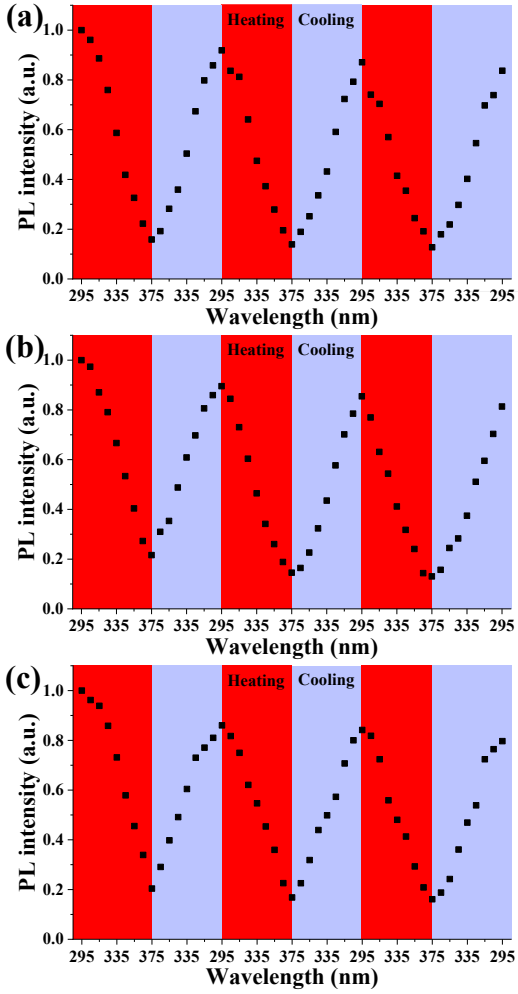


**Fig. S15** Thermal cycling measurements for (a) $CsPbI_3$@$SiO_2$ NCs, (b) $CsPbI_3$@$Ta_2O_5$ NCs and (c) $CsPbI_3$@$ZrO_2$ NCs. The integrated PL intensity is normalized to the initial value.

**Table S1** PLQY for $CsPbX_3$ NCs and $CsPbX_3$@Oxide core-shell NCs.

| Sample | PLQY | Sample | PLQY |
|---|---|---|---|
| $CsPbI_3$ | 66.9% | $CsPbBr_3$ | 85.3% |
| $CsPbI_3@SiO_2$ | 51.1% | $CsPbBr_3@SiO_2$ | 66.9% |
| $CsPbI_3@Ta_2O_5$ | 57.7% | $CsPbCl_3$ | 1.22% |
| $CsPbI_3@ZrO_2$ | 59.7% | $CsPbCl_3@SiO_2$ | 1.03% |